

A while at  $-100\text{ }^{\circ}\text{C}$ , the freezing point of methanol, the population of the molecules in this conformation increases to  $\sim 90\%$ . This result suggests that under the conditions in which solutions of spin-labeled methyl L-alanate were prepared for ENDOR studies the molecules are found predominantly in one conformation and that the ENDOR results, thus, describe primarily a single conformation. It is, therefore, of some interest to note that this conformer designated A in Figure 8 corresponds closest not only to the  $\phi, \psi$  dihedral angles characteristic of a right-handed  $\alpha$ -helix but also to the classical Z conformer of an ester group, which is of lower energy than its corresponding E rotamer.<sup>28</sup>

Registry No. I, 125109-37-7; II, 125109-38-8; III, 125137-89-5; IV, 125109-39-9; V, 125109-40-2; VI, 125109-41-3; H-Ala-OH, 56-41-7; L-H<sub>2</sub>NCD(CD<sub>3</sub>)COOH, 18806-29-6; L-H<sub>2</sub>NCD(CH<sub>3</sub>)COOH, 21386-65-2; L-H<sub>2</sub>NCH(CD<sub>3</sub>)COOH, 63546-27-0; H-Ala-OMe-HCl, 2491-20-5; L-H<sub>2</sub>NCD(CD<sub>3</sub>)COOMe-HCl, 125109-42-4; L-H<sub>2</sub>NCD(CH<sub>3</sub>)COOC-D<sub>3</sub>-HCl, 125109-43-5; L-H<sub>2</sub>NCH(CD<sub>3</sub>)COOCD<sub>3</sub>-HCl, 125109-44-6; L-H<sub>2</sub>NCD(CD<sub>3</sub>)COOCD<sub>3</sub>-HCl, 125109-45-7; 2,2,5,5-tetramethyl-1-oxypyrroline-3-carboxylic acid, 2154-67-8; 2,2,5,5-(<sup>2</sup>H<sub>12</sub>)tetramethyl-1-oxo-4-(<sup>2</sup>H)pyrroline-3-carboxylic acid, 88168-79-0.

(28) Wiberg, K. B.; Laidig, K. E. *J. Am. Chem. Soc.* **1987**, *109*, 5935-5943.

## Structure and Conformation of Spin-Labeled Amino Acids in Frozen Solutions Determined by Electron Nuclear Double Resonance. 2. Methyl *N*-(2,2,5,5-Tetramethyl-1-oxypyrrolinyl-3-carbonyl)-L-tryptophanate, a Molecule with Multiple Conformations<sup>1a</sup>

Gregg B. Wells,<sup>1b</sup> Devkumar Mustafi, and Marvin W. Makinen\*

Contribution from the Department of Biochemistry and Molecular Biology, The University of Chicago, Cummings Life Science Center, 920 East 58th Street, Chicago, Illinois 60637.

Received June 7, 1989

**Abstract:** The conformation of methyl *N*-(2,2,5,5-tetramethyl-1-oxypyrrolinyl-3-carbonyl)-L-tryptophanate in frozen solutions has been determined by application of electron nuclear double resonance (ENDOR) spectroscopy and computer-based molecular modeling. ENDOR spectra of methyl L-tryptophanate and of the corresponding methyl esters of  $\beta$ -fluoro- and  $\eta$ -2-fluorotryptophan acylated at the amino group with the spin-label 2,2,5,5-tetramethyl-1-oxypyrroline-3-carboxylic acid exhibited well-resolved resonance absorptions from protons and fluorines of the amino acid moiety. The ENDOR shifts were shown to correspond to principal hyperfine coupling (hfc) components, from which the dipolar contributions were estimated to calculate electron-nucleus separations. The ENDOR data indicated that there are two distinct conformations of spin-labeled methyl tryptophanate, the relative populations of which were dependent on solvent polarity. Torsion angle search calculations constrained by the ENDOR data showed that the predominant conformation in methanol was similar to that of a classical *g*<sup>-</sup> rotamer ( $\chi_1 \sim -63^\circ$ ) with a near perpendicular ( $\chi_2 \sim +105^\circ$ ) orientation of the indole ring. The second conformer was characterized by  $\chi_1 \sim -95^\circ$  and  $\chi_2 \sim -105^\circ$ , indicative of an antiperpendicular orientation. In chloroform/toluene only the antiperpendicular conformer was detected. The different solvent-dependent orientations of the indole ring with respect to the nitroxyl group are explained on the basis of dipolar interactions of the aromatic side chain with solvent and with the peptide bond.

The structure and conformation of amino acids and peptides in solution are of considerable importance in biophysical studies since the distribution of the side-chain dihedral angles is far from random and preferred conformations of amino acid side chains are frequently observed in proteins.<sup>2</sup> In general, the conformational analysis of amino acid and peptide derivatives in solution has been carried out on the basis of circular dichroism, infrared spectroscopy, nuclear magnetic resonance (NMR<sup>3</sup>), and potential energy calculations. Analysis of direct structural data obtained by NMR methods depends primarily on estimates of the vicinal, through-bond coupling constants of H <sup>$\alpha$</sup>  with the peptide amide proton H<sup>N</sup> or on estimates of coupling constants of protons bonded to adjacent carbons along the side chain.<sup>4</sup> Reliable estimates of

the vicinal coupling constants are difficult to obtain, and the data must be analyzed for multiple conformations, the relative populations of which are not estimated with high precision. In addition, such NMR data are often not analyzed further to determine whether the resonances derive from distinct conformers or whether they derive from multiple conformers that are in rapid equilibrium with each other on the NMR time scale. Also, there are little data to specify internucleus distances on which basis the conformational analysis would be significantly strengthened.

A variety of important problems in chemistry and biochemistry revolve around the relative conformational analysis of molecular structure. To this end we have found that electron nuclear double resonance (ENDOR<sup>3</sup>) spectroscopy can be incisively applied to assign structure and conformation of molecules in solution. In the accompanying publication<sup>5</sup> we demonstrated on the basis of ENDOR and molecular modeling that a nitroxyl spin-labeled derivative of L-alanine exhibits only one preferred conformation. In this communication we extend this approach to investigate the conformational properties of L-tryptophan, an amino acid that is expected to exhibit multiple conformations in solution.<sup>6,7</sup> We

(1) (a) This work was supported by a grant from the National Institutes of Health (GM 21900). (b) Supported in part by an MSTP Training Grant from the National Institutes of Health (GM 07281).

(2) (a) Chandrasekaran, R.; Ramachandran, G. N. *Int. J. Protein Res.* **1970**, *2*, 223-233. (b) Chothia, C. *Annu. Rev. Biochem.* **1984**, *53*, 537-572.

(3) The following abbreviations are used: EPR, electron paramagnetic resonance; ENDOR, electron nuclear double resonance; hf, hyperfine; hfc, hyperfine coupling; NMR, nuclear magnetic resonance; rf, radio frequency.

(4) (a) Feeney, J. *Proc. R. Soc. London, A* **1975**, *345*, 61-72. (b) Wüthrich, K. *NMR of Proteins and Nucleic Acids*; John Wiley & Sons: New York, 1986; p 292. (c) Wüthrich, K. *Acc. Chem. Res.* **1989**, *22*, 36-44.

(5) Mustafi, D.; Sachleben, J. R.; Wells, G. B.; Makinen, M. W. *J. Am. Chem. Soc.*, preceding article in this issue.

demonstrate that there are two rotamer conformations of the side chain in methyl *N*-(2,2,5,5-tetramethyl-1-oxypyrrolinyl-3-carbonyl)-L-tryptophanate, the relative populations of which are strikingly dependent on solvent polarity. We show that the different conformers can be distinguished on the basis of ENDOR spectra and that one of the conformers corresponds closely to that of methyl *N*-acetyl-L-tryptophanate in crystals.<sup>8</sup> We also provide a detailed description of their three-dimensional structures.

### Experimental Procedures

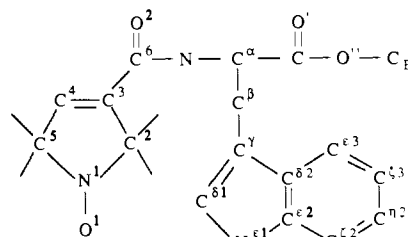
**General Materials.** Organic solvents and reagents were employed as described in the preceding publication.<sup>5</sup> Acylase I from *Aspergillus* was obtained from Sigma Chemical Co. (St. Louis, MO 63178). Fluorinated D,L-tryptophan derivatives and L- and D-tryptophan were obtained from Aldrich Chemical Co., Inc. (Milwaukee, WI 53233). Specifically labeled D,L-( $\alpha,\beta,\beta$ -<sup>2</sup>H<sub>3</sub>)-, L-(indolyl-<sup>2</sup>H<sub>5</sub>)-, and D,L-( $\alpha,\beta,\beta$ -indolyl-<sup>2</sup>H<sub>8</sub>)tryptophan derivatives were obtained from MSD Isotopes (St. Louis, MO 63116). Deuteriated solvents and reagents were obtained from Cambridge Isotope Laboratories, Inc. (Woburn, MA 01801).

**L-( $\alpha$ -<sup>2</sup>H)Tryptophan.** Upson and Hruby<sup>9</sup> reported a general method for the preparation of ( $\alpha$ -<sup>2</sup>H)-substituted amino acids. Because of the sensitivity of tryptophan to hot acid, a modification of their method was used for preparation of L-( $\alpha$ -<sup>2</sup>H)tryptophan. D-tryptophan (3 g, 0.015 mol) was shaken for 1 h in 15 mL of <sup>2</sup>H<sub>2</sub>O at room temperature. The amino acid was recovered by removal of <sup>2</sup>H<sub>2</sub>O by evacuation and was added to a solution of 50 mL of (<sup>2</sup>H<sub>4</sub>)acetic acid containing 5 mL of (<sup>2</sup>H<sub>6</sub>)acetic anhydride. The mixture was heated to 80 °C for 2 min, cooled to 40 °C, and stirred at this temperature for 2 days. The acetic acid and unreacted acetic anhydride were removed in vacuo. The residue of *N*-acetyl-D,L-( $\alpha$ -<sup>2</sup>H)tryptophan<sup>10</sup> was dissolved in <sup>2</sup>H<sub>2</sub>O, made alkaline with NaOH, and then recrystallized by addition of 0.5 M <sup>2</sup>HCl.

All of the recrystallized *N*-acetyl-D,L-( $\alpha$ -<sup>2</sup>H)tryptophan was dissolved in 25 mL of <sup>2</sup>H<sub>2</sub>O. A 5-mL solution of 0.075 g of acylase I in <sup>2</sup>H<sub>2</sub>O was added, the nominal pH was adjusted to 7.1, and the mixture was kept at 35 °C for 3 days. The pH of the mixture was then adjusted at room temperature to 6.0 and the solvent removed by evacuation until the appearance of crystals of L-( $\alpha$ -<sup>2</sup>H)tryptophan. The mixture was then further chilled at 0 °C for 1 h, and crystalline L-( $\alpha$ -<sup>2</sup>H)tryptophan was recovered by filtering and washing with cold <sup>2</sup>H<sub>2</sub>O. The yield was 0.69 g (46%); mp 260–263 °C with decomposition. Deuterium exchange at the C $\alpha$  atom was assessed by NMR to be greater than 90%.

**Methyl L-Tryptophanate Hydrochloride.** The synthesis of methyl L-tryptophanate hydrochloride followed closely that described for methyl L-alanate hydrochloride.<sup>5</sup> To 3 mL of methanol was added 0.072 mL of H<sub>2</sub>O. The solution was cooled to 0 °C, and 0.70 mL of colorless, doubly distilled SOCl<sub>2</sub> was added. The mixture was warmed to room temperature, 0.35 g of L-tryptophan was added, and the mixture was warmed to 60 °C for 40 min, during which time the product precipitated. The solvent was removed in vacuo and the product was washed several times with fresh methanol. The product, generally in excess of 90% yield, was used without further purification (mp 220–223 °C). Anal. Calcd (Found): C, 56.58 (56.28); H, 5.94 (6.00); N, 11.00 (10.92); Cl, 13.92 (13.92). Methyl esters of fluorinated tryptophan derivatives were prepared in a similar manner and showed comparable yields and purity according to elemental analysis, melting point, and NMR spectra.

**Methyl *N*-(2,2,5,5-Tetramethyl-1-oxypyrrolinyl-3-carbonyl)-L-tryptophanate (I).** We describe a typical procedure for the coupling of the spin-label to the amine group of tryptophan. In 10 mL of dry methylene chloride was dissolved 0.15 g (0.81 mmol) of 2,2,5,5-tetramethyl-1-oxypyrrolinyl-3-carboxylic acid with 0.14 g (0.86 mmol) of carbonyl-1,1'-diimidazole (Aldrich). After 15 min, 0.21 g (0.81 mmol) of methyl L-tryptophanate hydrochloride was added to the mixture. This dissolved upon addition of 0.12 mL (0.85 mmol) of multiply distilled triethylamine. The reaction mixture was maintained at room temperature for 2 days,



- I. SL (<sup>2</sup>H<sub>3</sub>)methyl L-tryptophanate
- II. SL (<sup>2</sup>H<sub>3</sub>)methyl D, L-( $\zeta$ -F)-tryptophanate
- III. SL (<sup>2</sup>H<sub>3</sub>)methyl D, L-( $\eta$ -F)-tryptophanate
- IV. SL (<sup>2</sup>H<sub>3</sub>)methyl L-(indolyl-<sup>2</sup>H<sub>5</sub>)-tryptophanate
- V. SL methyl L-(indolyl-<sup>2</sup>H<sub>5</sub>)-tryptophanate
- VI. SL (<sup>2</sup>H<sub>3</sub>)methyl L-( $\alpha$ -<sup>2</sup>H)-tryptophanate
- VII. SL (<sup>2</sup>H<sub>3</sub>)methyl D, L-( $\alpha,\beta,\beta$ -<sup>2</sup>H<sub>3</sub>)-tryptophanate
- VIII. SL (<sup>2</sup>H<sub>3</sub>)methyl D, L-( $\alpha,\beta,\beta$ -<sup>2</sup>H<sub>3</sub>-indolyl-<sup>2</sup>H<sub>5</sub>)-tryptophanate

**Figure 1.** Illustration of the chemical bonding structure and the atomic numbering scheme of specifically fluorinated and deuteriated analogues of methyl *N*-(2,2,5,5-tetramethyl-1-oxypyrrolinyl-3-carbonyl)tryptophanate employed in this study. SL refers to the spin-label acyl moiety attached to the amine nitrogen atom.

diluted with 15 mL of methylene chloride, washed four times with 75 mL of 0.1 N HCl, washed twice with 75 mL of 5% (w/v) NaHCO<sub>3</sub>, and finally washed to neutrality with H<sub>2</sub>O. The organic layer was dried over MgSO<sub>4</sub>. Removal of the organic layer in vacuo left a yellow oil that solidified from a mixture of methylene chloride/petroleum ether. Yields of the spin-labeled methyl tryptophanate were typically ~25% of theoretical. For spin-labeled methyl L-tryptophanate (mp 70–75 °C) elemental analysis showed the following. Anal. Calcd (Found): C, 65.61 (64.87); H, 6.82 (6.65); N, 10.93 (11.09).

The series of deuteriated and fluorinated analogues of spin-labeled methyl tryptophanate employed in this investigation is shown in Figure 1. Comparable results with respect to yield and elemental analysis for synthesis of II–VIII were obtained as described above for the synthesis of I.

**EPR and ENDOR.** Spectroscopic studies were carried out as described in the preceding publication.<sup>5</sup> All spin-labeled derivatives were dissolved in  $5 \times 10^{-3}$  M concentration in (<sup>2</sup>H<sub>4</sub>)methanol or 50:50 (v/v) (<sup>2</sup>H)chloroform/(<sup>2</sup>H<sub>8</sub>)toluene. For description of experimental results, the settings A and B of the static laboratory magnetic field refer to the low-field and central-field EPR absorption components of the nitroxyl moiety, respectively, as defined in the accompanying publication.<sup>5</sup> ENDOR spectra were collected under conditions of ~8-kHz modulation depth of the rf field and at sample temperatures of ~40 K, as described previously.<sup>5</sup> The method of interpreting ENDOR spectra for spin-labeled molecules in terms of principal dipolar hfc values and electron–nucleus distances has been presented elsewhere.<sup>5,12</sup>

**Molecular Modeling.** The molecular model of I was constructed from X-ray-defined molecular fragments derived from 2,2,5,5-tetramethyl-1-oxypyrrolinyl-3-carboxamide<sup>13</sup> and methyl *N*-acetyl-L-tryptophanate<sup>8</sup> by least-squares superpositioning the C(3), C(6), O(2), and N atoms derived from the spin-label carboxamide onto the CH<sub>3</sub>, C, O, and N atoms of the *N*-acetyl moiety of methyl *N*-acetyl-L-tryptophanate. The superpositioning yielded a root-mean-square deviation of 0.012 Å for the four atoms. Molecular modeling and torsional search calculations were carried out with use of the programs SYBYL<sup>14a-c</sup> and INSIGHT<sup>14d</sup> running on an Evans & Sutherland PS390 graphics terminal with a host VAX3500 computer.

(6) (a) Dezube, B.; Dobson, C. M.; Teague, C. E. *J. Chem. Soc. Perkin Trans. 2* **1981**, 730–735. (b) Levine, B. A.; Williams, R. J. P. *Proc. R. Soc. London, A* **1975**, 345, 5–22.

(7) (a) Cavanaugh, J. R. *J. Am. Chem. Soc.* **1970**, 92, 1488–1493. (b) Skrabal, P.; Rizzo, V.; Baici, A.; Bangerter, F.; Luisi, P. L. *Biopolymers* **1979**, 18, 995–1008. (c) Baici, A.; Rizzo, V.; Skrabal, P.; Luisi, P. L. *J. Am. Chem. Soc.* **1979**, 101, 5170–5178.

(8) Cotrait, P. M.; Barrans, Y. *Acta Crystallogr., Sect. B* **1974**, 30, 510–513.

(9) Upson, D. A.; Hruby, V. J. *J. Org. Chem.* **1977**, 42, 2329–2330.

(10) The reaction with acetic acid and acetic anhydride is known to result in racemization of the amino acid.<sup>11</sup>

(11) Greenstein, J. P.; Winitz, M. *Chemistry of the Amino Acids*; R. E. Krieger Publishing Co.: Malabar, FL, 1984; Vol. 3, pp 2344–2345.

(12) Wells, G. B.; Makinen, M. W. *J. Am. Chem. Soc.* **1988**, 110, 6343–6352.

(13) Turley, J. W.; Boer, F. P. *Acta Crystallogr., Sect. B* **1972**, 28, 1641–1644.

(14) (a) Marshall, G. R., personal communication. (Detailed information on the use of this program package can be obtained from Tripos Associates, Inc., 1600 S. Hanley Road, St. Louis, MO 63144.) (b) Naruto, S.; Motoc, J.; Marshall, G. R.; Daniels, S. B.; Sofia, M. J.; Katzenellenbogen, J. A. *J. Am. Chem. Soc.* **1985**, 107, 5262–5270. (c) Iijima, H.; Dunbar, J. B., Jr.; Marshall, G. R. *Proteins: Struct., Funct., Genet.* **1987**, 2, 330–339. (d) Dayringer, H. E.; Tramontano, A.; Sprang, S. R.; Fletterick, R. J. *J. Mol. Graphics* **1986**, 4, 82–87.

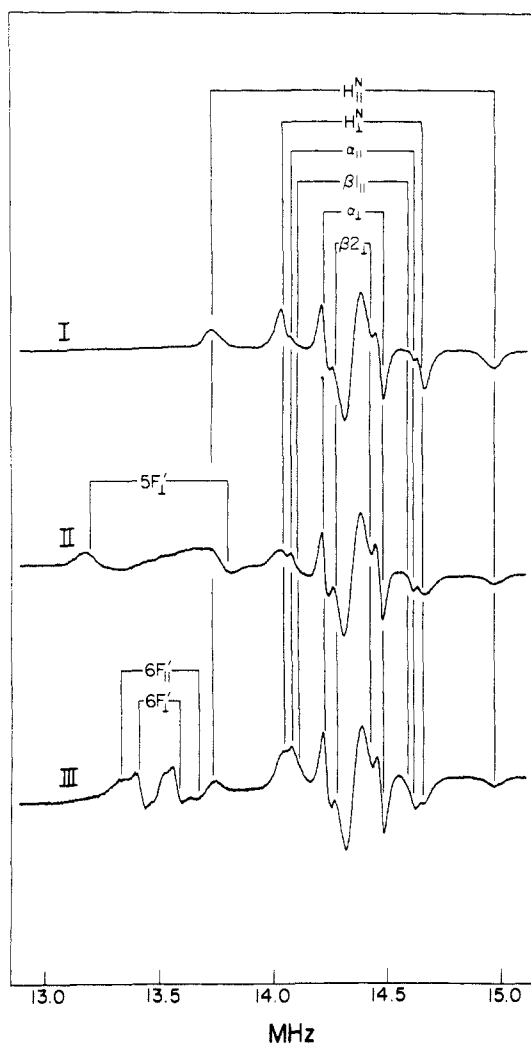


**Figure 2.** Proton and fluorine ENDOR spectra of I-III in ( $^2\text{H}$ )chloroform/ $(^2\text{H}_8)$ toluene with  $\text{H}_0$  at position B. The ENDOR absorption features are indicated in each spectrum for each class of nuclei and are symmetrically spaced about their respective Larmor frequencies of 13.48 MHz for  $\nu_{\text{F}}$  and 14.33 MHz for  $\nu_{\text{H}}$ . The ENDOR splittings that correspond to principal hfc components are identified by the stick diagrams. The ENDOR absorption features for fluorines attached to the  $\text{C}^{\beta 3}$  and  $\text{C}^{\beta 2}$  positions of the indole ring are labeled as  $5\text{F}'$  and  $6\text{F}'$ , respectively.

## Results

**A. ENDOR of Spin-Labeled Methyl Tryptophanate in a Nonpolar Solvent.** In Figure 2 are illustrated the proton and fluorine ENDOR spectra of I-III dissolved in perdeuterated chloroform/toluene. For this  $\text{H}_0$  setting, both parallel and perpendicular hfc components are generally observed in the ENDOR spectrum. The spectra show that the proton resonance absorptions centered about 14.33 MHz are well separated from the resonance absorptions of the fluorine substituents centered about 13.48 MHz, except for overlapping of the high-frequency resonance absorption of the fluorine substituent of II with the parallel resonance absorption belonging to  $\text{H}^{\text{N}}$ . The spectrum of the fluorine resonance feature of II is sufficiently distinct, nonetheless, to estimate accurately the  $^{19}\text{F}$  hf splitting. The ENDOR absorption features observed for the fluorine substituent of II were also observed for setting A of the static laboratory magnetic field, and on this basis, we have assigned this pair of features as the perpendicular hfc components of the  $^{19}\text{F}$  substituent. On the low-frequency side, we have been unable to identify the parallel hfc component of the fluorine substituent of II, probably because of its low amplitude. In addition, the higher frequency parallel hfc component is buried by more intense, overlapping proton resonance features. On the other hand, both the parallel and perpendicular hfc components were observed for the  $^{19}\text{F}$  substituent of III, and their assignments

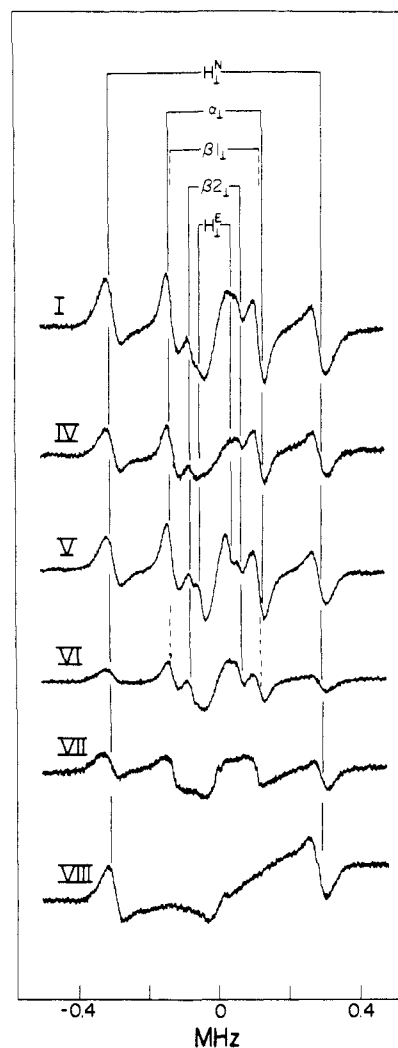


**Figure 3.** Proton ENDOR spectra of I and IV-VIII in ( $^2\text{H}$ )chloroform/ $(^2\text{H}_8)$ toluene with  $\text{H}_0$  set to the low-field absorption (setting A) of the spin-label EPR spectrum. The abscissa indicates the ENDOR shift (measured ENDOR frequency minus free nuclear Larmor frequency). The ENDOR absorption features are symmetrically spaced about the proton Larmor frequency of 14.19 MHz. The ENDOR splittings for  $\text{H}^{\text{N}}$ ,  $\text{H}^{\alpha}$ ,  $\text{H}^{\beta 1}$ ,  $\text{H}^{\beta 2}$ , and  $\text{H}^{\text{E}}$  are identified in the stick diagram.

were verified by the dependence of the ENDOR spectrum with change of  $\text{H}_0$  from setting B to setting A. The proton resonances of II and III appeared at identical frequencies as for the parent spin-labeled methyl L-tryptophanate. This observation requires that the fluorine-substituted derivatives and the parent compound exhibit identical conformations in solution. Although both parallel and perpendicular hfc components of  $\text{H}^{\alpha}$  and  $\text{H}^{\text{N}}$  are observed for the magnetic field setting in Figure 2, such is not the case for  $\text{H}^{\beta 1}$  and  $\text{H}^{\beta 2}$ . The identification and assignment of resonance features for  $\text{H}^{\beta 1}$  and  $\text{H}^{\beta 2}$  are described in more detail below.

In Figure 3 are illustrated the hfc components of specific classes of protons of I, which can be assigned on the basis of deuteration. Since  $\text{H}_0$  was set to the low-field absorption of the EPR spectrum (setting A), the spectra in Figure 3 identify only the perpendicular hfc components of each class of protons. The resonance features of  $\text{H}^{\text{N}}$  are identified in the spectrum of VIII. Identical features are observed in the other spectra. The resonance features of  $\text{H}^{\alpha}$  are identified in Figure 3 by comparison of the spectra of I and IV-VI. However, comparison of the spectra of V and VI shows a weak resonance feature in the spectrum of VI that is overlapping with the resonance of  $\text{H}^{\alpha}$  and is not ascribable to incomplete deuteration. When this feature was resolved in scans at higher resolution, it exhibited slightly smaller ENDOR splittings than for the more intense, overlapping feature observed in the spectra of I, IV, and V. Since a clearly resolved feature in the spectra

**Table I.** Summary of hfc Components and Estimated Electron-Nucleus Distances in Methyl *N*-(2,2,5,5-Tetramethyl-1-oxypyrrolinyl-3-carbonyl)-L-tryptophanate in Frozen (<sup>2</sup>H)Chloroform/(<sup>2</sup>H<sub>8</sub>)Toluene

nucleus and position	hfc components, MHz					<i>r</i> , <sup>a</sup> Å
	<i>A</i> <sub>  </sub>	<i>A</i> <sub>⊥</sub>	<i>A</i> <sub>iso</sub>	<i>A</i> <sub>  </sub> <sup>D</sup>	<i>A</i> <sub>⊥</sub> <sup>D</sup>	
H <sup>N</sup>	1.203	0.606	-0.003	1.206	-0.603	5.08 ± 0.04
H <sup>α</sup>	0.539	0.257	0.008	0.531	-0.265	6.68 ± 0.08
H <sup>β1</sup>	0.458	0.232	-0.002	0.460	-0.230	7.01 ± 0.10
H <sup>β2</sup>		0.144			-0.144	8.20 ± 0.18
H <sup>E</sup>		0.088			-0.088	9.67 ± 0.35
F <sup>β3</sup>		0.592			-0.592	5.01 ± 0.14
F <sup>γ2</sup>	0.335	0.179	-0.008	0.343	-0.171	7.58 ± 0.12

<sup>a</sup>Uncertainty in frequency of 0.015–0.020 MHz due to the line width of each absorption is included in the calculation of electron-nucleus distances.

of I and IV–VI can be assigned to an H<sup>β</sup> proton (labeled β2 in the diagram), we ascribe the overlapping feature with H<sup>α</sup> to the other H<sup>β</sup> proton. Finally the resonance features of the OCH<sub>3</sub> group are identified by comparison of the spectra of IV with that of V.

With H<sub>0</sub> at setting B, a set of resonance features similar to those in Figure 3 was observed together with their corresponding parallel hfc components. However, for this setting, parallel hfc features ascribable to H<sup>β2</sup> and to the OCH<sub>3</sub> group could not be clearly identified, presumably because they are overlapping with other absorptions of greater intensity.

The broad, central resonance absorption feature in the spectrum of VII, when compared to the spectrum of VIII in Figure 3, shows that this feature is ascribable to protons of the indole ring. The overlapping absorption characteristics of these protons, however, prevent their assignment to specific positions in the indole ring and prevent, therefore, their use for assignment of side-chain conformation. We, therefore, have had to employ fluorine substituents as a spectroscopic probe of side-chain conformation.

In Table I we have summarized the values of the parallel and perpendicular hfc components for each class of protons and fluorine substituents of spin-labeled tryptophanate esters in (<sup>2</sup>H)chloroform/(<sup>2</sup>H<sub>8</sub>)toluene. We have also included in Table I the estimated dipolar hfc components and the corresponding calculated electron-nucleus separations *r*. As seen in the accompanying publication,<sup>5</sup> the isotropic coupling contributions of the H<sup>β1</sup>, H<sup>β2</sup>, and OCH<sub>3</sub> nuclei are essentially negligible. Therefore, we have calculated the corresponding values of *r* for these two classes of nuclei only on the basis of their observed perpendicular hfc components as seen in Figures 2 and 3 and tabulated in Table I.

**B. ENDOR of Spin-Labeled Methyl Tryptophanate in a Polar Solvent.** Figure 4 compares the <sup>19</sup>F ENDOR spectrum of II in perdeuteriated chloroform/toluene and methanol. The spectrum of II in chloroform/toluene is identical with that in Figure 2 in the 13.5-MHz region and is dominated by broad resonance features. On the other hand, the spectrum of II in methanol exhibits additional resonances near the <sup>19</sup>F Larmor frequency, which are essentially absent in the chloroform/toluene system. The broad <sup>19</sup>F resonances of II in methanol with splittings identical with those in the chloroform/toluene solvent are of diminished peak-to-peak amplitude. Comparable spectral differences dependent on solvent composition were also observed for III. The new resonances for II and III in methanol, which are essentially absent in chloroform/toluene, together with the change in the peak-to-peak intensity, indicate the presence of at least two conformers differing in their electron-fluorine separations.

Although the ENDOR splittings of the resonance features belonging to H<sup>α</sup> were nearly identical in both solvent systems, the splittings belonging to H<sup>β1</sup> and H<sup>β2</sup> showed small changes that indicated corresponding differences in their respective electron-proton separations. This observation confirms the assignment of the two sets of <sup>19</sup>F resonances in Figure 4 to different molecular conformers. We have summarized in Table II the values of the principal hfc components of each class of protons in this second

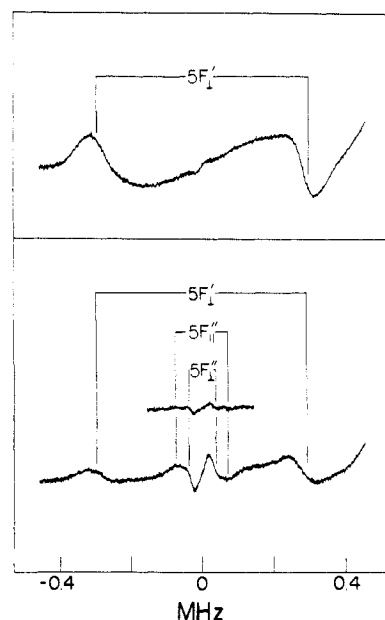


**Figure 4.** Fluorine ENDOR spectra of II in (<sup>2</sup>H)chloroform/(<sup>2</sup>H<sub>8</sub>)toluene (top) and in (<sup>2</sup>H<sub>4</sub>)methanol (bottom) with H<sub>0</sub> at position B of the EPR spectrum. Two sets of fluorine resonances (F', F'') are identified in the stick diagrams, as recorded for 8-kHz modulation depth of the rf field. In the lower panel the upper spectrum was recorded with a modulation depth of 7 KHz in order to demonstrate that the two sets of features remain separable spectroscopically. Other conditions are as in Figure 2.

**Table II.** Summary of hfc Components and Estimated Electron-Nucleus Distances in Methyl *N*-(2,2,5,5-Tetramethyl-1-oxypyrrolinyl-3-carbonyl)-L-tryptophanate in Frozen (<sup>2</sup>H<sub>4</sub>)Methanol

nucleus and position	hfc components, MHz					<i>r</i> , <sup>a</sup> Å
	<i>A</i> <sub>  </sub>	<i>A</i> <sub>⊥</sub>	<i>A</i> <sub>iso</sub>	<i>A</i> <sub>  </sub> <sup>D</sup>	<i>A</i> <sub>⊥</sub> <sup>D</sup>	
H <sup>N</sup>		0.593			-0.593	5.11 ± 0.06
H <sup>α</sup>	0.536	0.256	0.008	0.528	-0.264	6.70 ± 0.07
H <sup>β1</sup>	0.370	0.184	-0.001	0.369	-0.185	7.54 ± 0.08
H <sup>β2</sup>		0.139			-0.139	8.29 ± 0.30
H <sup>E</sup>		0.107			-0.107	9.05 ± 0.22
F <sup>β3</sup>	0.152	0.073	0.002	0.150	-0.075	10.10 ± 1.02
F <sup>γ2</sup>		0.598			-0.598	5.00 ± 0.10 <sup>b</sup>
F <sup>γ2</sup>	0.130	0.071	-0.004	0.134	-0.067	10.22 ± 1.02
F <sup>γ2</sup>	0.345	0.181	-0.005	0.340	-0.176	7.54 ± 0.33 <sup>b</sup>

<sup>a</sup>Uncertainty in frequency of 0.015–0.025 MHz is included in the calculation of electron-nucleus distances. <sup>b</sup>Refers to the second conformation observed in methanol, which is identical with the predominant conformation in chloroform/toluene as indicated in Table I.

conformer of spin-labeled methyl tryptophanate in methanol as well as for the principal hfc components of the fluorine substituents in both conformers. We have also listed the electron-nucleus separations *r* calculated on the basis of the estimated dipolar hfc components.

**C. Molecular Modeling of Spin-Labeled Methyl L-Tryptophanate.** We have previously pointed out that the coordinates of the effective electronic point dipole of the nitroxyl group may vary slightly along the N–O bond, depending on solvent polarity.<sup>5,12</sup> To determine the influence of the change in polarity on the position of the effective point dipole along the N–O bond for the two solvent systems employed in this study, we have measured the isotropic <sup>14</sup>N hfc of I also in chloroform/toluene. This measurement yielded a value of 14.80 ± 0.03 G for *a*<sub>N</sub> compared to that of 14.96 G in methanol. This difference results in a calculated change of less than 0.01 Å in the position of the effective electronic dipole along the N–O bond. Since this difference has no perceptible influence on the evaluation of the conformational properties of the spin-labeled molecule because of the angle increment feasible in torsion angle search calculations, we have consequently employed identical

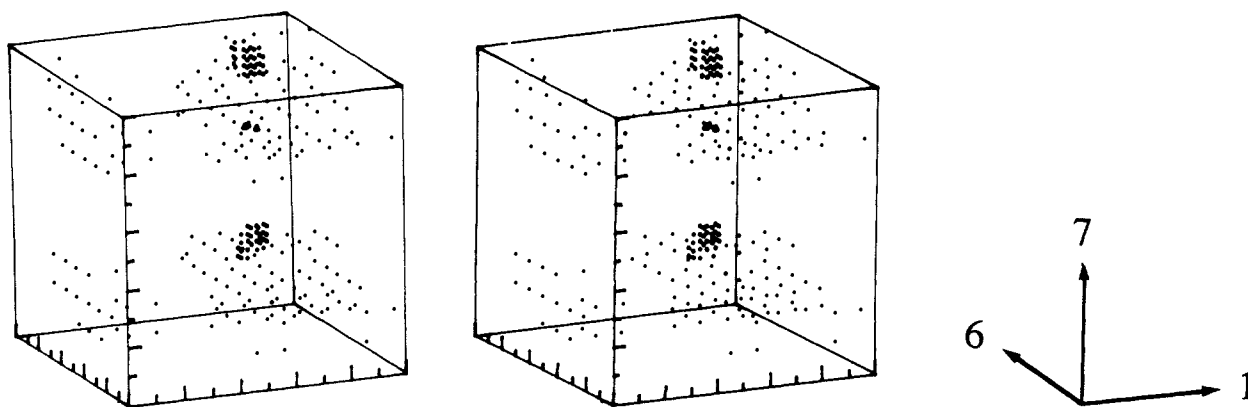


**Figure 5.** Stereo diagram of the angle map of spin-labeled methyl L-tryptophanate. The axes 1, 6, and 7 represent 0–360° rotation around the N–C $\alpha$ , C $\alpha$ –C $\beta$ , and C $\beta$ –C $\gamma$  bonds, respectively. The low-density dots represent conformational space that is compatible with nonbonded van der Waals constraints. The symmetrically positioned pair of high-density dots identify two families of rotamers that belong to the “extended” conformation. The small circumscribed set of high-density dots refers to the “closed” structure and defines an essentially unique conformation of the molecule in the chloroform/toluene solvent system.

coordinates of the effective point dipole of the nitroxyl group for both solvent systems. This position corresponds to that established for methyl *N*-(2,2,5,5-tetramethyl-1-oxypyrrolinyl-3-carbonyl)-L-alanate in methanol.<sup>5</sup>

The molecular model of spin-labeled methyl L-tryptophanate was constructed by superpositioning the C(3), C(6), O(2), and N atoms derived from 2,2,5,5-tetramethyl-1-oxypyrrolinyl-3-carboxamide<sup>13</sup> onto the *N*-acetyl moiety of methyl *N*-acetyl-L-tryptophanate.<sup>8</sup> To determine the conformations of spin-labeled methyl L-tryptophanate as observed for both solvent systems, we have carried out a conformational search of the limits of the torsion angles for rotation around the C(3)–C(6) and C(6)–N bonds within the spin-label acyl moiety and around the N–C $\alpha$ , C $\alpha$ –C $\beta$ , C $\beta$ –C $\gamma$ , C $\alpha$ –C, and C–O'' bonds within the tryptophanyl moiety, similar to our analysis of spin-labeled methyl L-alanate.<sup>5</sup> In contrast to the spectroscopic results of spin-labeled methyl L-alanate, the ENDOR data indicated two conformers of spin-labeled methyl tryptophanate of which the relative populations were dependent on solvent composition. We have correspondingly applied the two sets of ENDOR distance constraints separately, as summarized in Tables I and II. For purposes of modeling, we have carried out the conformational analysis only with respect to the L enantiomer of tryptophan although some of the ENDOR spectra were collected for racemic D,L mixtures. Identical results with respect to electron–nucleus separations would obtain for the D enantiomer.

The results of the conformational search for rotation around the N–C $\alpha$ , C $\alpha$ –C $\beta$ , and C $\beta$ –C $\gamma$  bonds are illustrated in Figure 5. The distance constraints for spin-labeled methyl tryptophanate in chloroform/toluene limit the number of ENDOR compatible conformations to a very small range, resulting in a nearly unique conformation of the amino acid side chain with respect to the spin-label moiety. However, for the molecule in methanol the calculations resulted in two regions of conformational space compatible with the ENDOR distance constraints. As will be shown below for the molecule in methanol, this difference affects only the orientation of the indole ring.

From such torsion angle search calculations, molecular models were constructed according to the mean values of the dihedral angles for each family of conformers. Least-squares superpositioning the N, C $\alpha$ , C $\beta$ , and C atoms of I onto the corresponding atoms of spin-labeled methyl L-alanate<sup>5</sup> yielded a difference of 0.37 and 0.16 Å in the position of C(6) for spin-labeled methyl tryptophanate in methanol and in chloroform/toluene, respectively, and a difference of 4° in the dihedral angle [C(3)–C(6)–N–C $\alpha$ ]. The orientation of the pyrrolinyl ring with respect to the peptide linkage and the backbone atoms of the amino acid moiety is, thus, essentially identical in both L-tryptophanate and L-alanate systems. This relationship is readily confirmed by the similar electron–proton separations of H<sup>N</sup> and H $\alpha$  in Tables I and II with those of methyl L-alanate.<sup>5</sup>

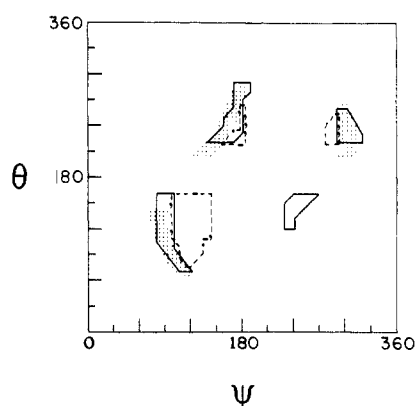


**Figure 6.** Comparison of torsion angle maps of the methyl carboxylate group of spin-labeled methyl L-tryptophanate and of methyl L-alanate. The axes labeled as  $\psi$  and  $\theta$  represent 0–360° rotation around the C $\alpha$ –C and C–O'' bonds, respectively. The conformational space compatible with the ENDOR distance constraint to the averaged ester methyl protons (H<sup>E</sup>) is represented by the closed solid line for spin-labeled methyl tryptophanate in methanol, by the dashed line for the molecule in chloroform/toluene, and by dots for spin-labeled methyl L-alanate.<sup>5</sup>

Figure 6 compares the angle map for the dihedral angles involving the C $\alpha$ –C and C–O'' bonds of spin-labeled methyl tryptophanate and alanate molecules. In both molecules, three distinct families of conformations of the methyl carboxylate group are found compatible with both nonbonded van der Waals constraints and the ENDOR-determined distance constraint to the ester methyl group. The three closely overlapping regions of conformational space in Figure 6 indicate that the methyl carboxylate conformations are similar in both types of spin-labeled amino acids. A small region, as shown in the angle map, was found compatible with the ENDOR data for the conformation of spin-labeled methyl tryptophanate in methanol that is not observed for the conformation in chloroform/toluene or for the alanate analogue. Since this region is calculated only for spin-labeled methyl tryptophanate in methanol, we believe that it represents a cumulative effect of the somewhat larger uncertainties associated with the distance constraints to H<sup>N</sup>, H<sup>B2</sup>, and H<sup>E</sup> in this case. Since the conformation of the methyl carboxylate group has been discussed in detail with respect to the alanate molecule<sup>5</sup> and similar conformations are found for the methyl tryptophanate analogue, we restrict further discussion to the structural relationships between the indole side chain and the pyrrolinyl ring.

#### Discussion

The molecular structures of each of the three conformations of spin-labeled methyl L-tryptophanate compatible with the ENDOR electron–nucleus separations are illustrated in Figure 7.

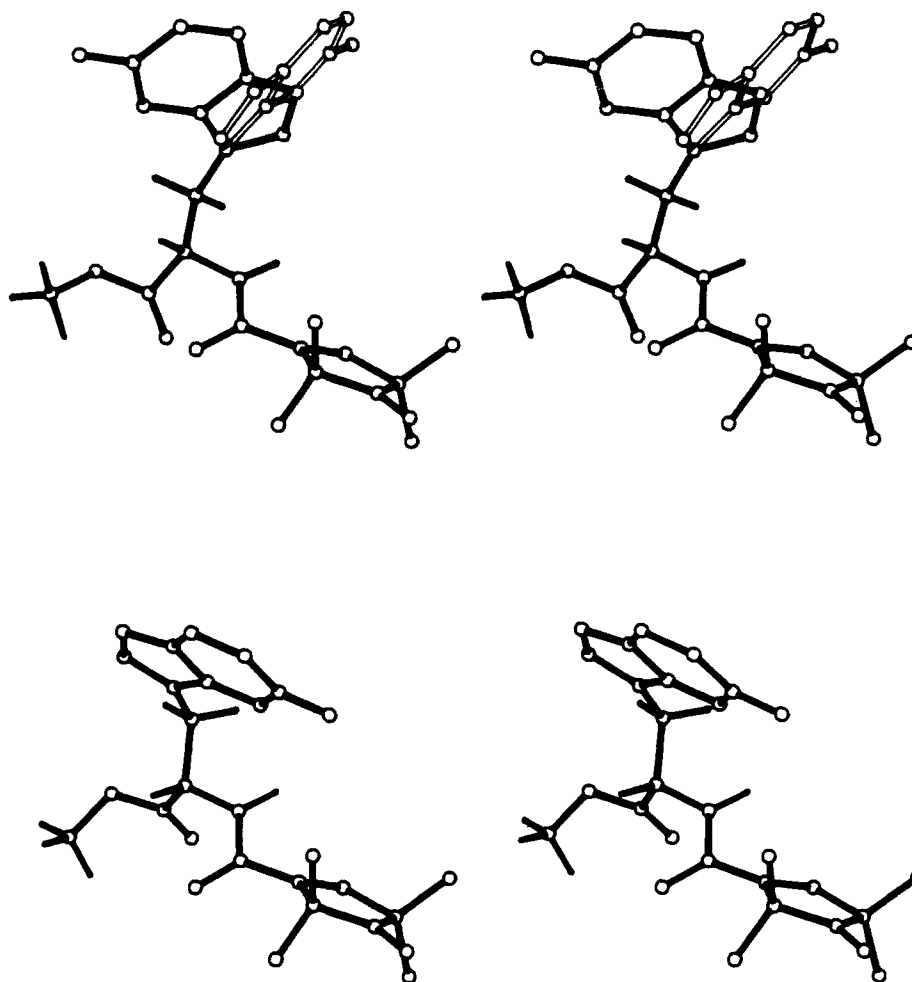


**Figure 7.** Stereo diagram of "extended" (upper) and "closed" (lower) conformations of spin-labeled methyl L-tryptophanate. The structures are drawn according to the mean values of the dihedral angles shown in Figure 5 and Table III. In the upper diagram the solid bonds correspond to the "extended" conformer A of Table III while the open bond structure is that of conformer B. The ENDOR significant hydrogens and the  $\zeta$ -fluorine substituent on the indole ring are shown in addition to the nonhydrogen atoms. The methyl carboxylate group is drawn according to the mean  $\psi, \theta$  dihedral angles of  $170^\circ, -120^\circ$ , respectively, corresponding to the upper left-hand area of  $\psi, \theta$  space indicated in Figure 6. These values correspond closest to those in methyl *N*-acetyl-L-tryptophanate.<sup>8</sup>

These structures correspond to the mean values of the dihedral angles obtained from torsion angle search calculations as illustrated in Figures 5 and 6. It is seen that the three structures differ primarily according to the relative orientation of the indole ring with respect to the spin-label moiety. We correspondingly designate the conformation of I with the longer electron-fluorine distance as "extended" while the conformation with the shorter electron-fluorine distance is designated as "closed". Since two "extended" conformations are compatible with the ENDOR data, we refer to them as conformers A and B, respectively. The "closed" conformation of the molecule is referred to as conformer C. Values of the dihedral angles of these three conformers of the spin-labeled methyl tryptophanate molecule as derived from ENDOR data are compared in Table III to those calculated on the basis of the molecular model constructed from X-ray-defined atomic coordinates of the pyrrolinylcarboxamide form of the spin label<sup>13</sup> and of methyl *N*-acetyl-L-tryptophanate.<sup>8</sup> The ENDOR constrained values of dihedral angles were calculated on the basis of estimates of  $r$  in Tables I and II while the uncertainties associated with each dihedral angle are evaluated from the ENDOR line widths.

The values of the dihedral angles about the C(6)-N bond for the three conformations found in this study show that the peptide linkage is essentially planar, in excellent agreement with the X-ray results. The tilt of the plane of the peptide group with respect to the pyrrolinyl ring is  $38.4^\circ$  in conformers A and B and  $48.4^\circ$  in conformer C. The carboxamide spin-label molecule in the crystal<sup>13</sup> is associated with a corresponding angle of  $29^\circ$  while

that for spin-labeled methyl L-alanate<sup>5</sup> is  $32^\circ$ . As indicated in Table III, the values of dihedral angles involving atoms of the nitroxyl group and extending up to the  $C^\beta$  atom for the three conformers of spin-labeled methyl L-tryptophanate are very similar to those of the spin-labeled alanate analogue,<sup>5</sup> indicating an essentially constant orientation of the nitroxyl ring with respect to the backbone and  $C^\beta$  atoms of the respective amino acid moieties. It is of interest to point out that for conformers A and B the dihedral angle [C(6)-N-C $^\alpha$ -C] that can be considered analogous to the dihedral angle  $\phi$  in dipeptide structures (cf., ref 5) is very close to that in methyl *N*-acetyl-L-tryptophanate.<sup>8</sup> This angle in conformer C differs substantially but is similar to the value found in spin-labeled methyl L-alanate. A similar relationship holds for the dihedral angle [C(6)-N-C $^\alpha$ -C $^\beta$ ].

The conformation of the side chain of tryptophan is generally described on the basis of two dihedral angles  $\chi_1$  and  $\chi_2$  defined as [N-C $^\alpha$ -C $^\beta$ -C $^\gamma$ ] and [C $^\alpha$ -C $^\beta$ -C $^\gamma$ -C $^\delta$ ], respectively, in Table III. The classical rotamers of  $\chi_1$  and  $\chi_2$  are diagrammatically illustrated in Figure 8. The predominant conformation of L-tryptophan in aqueous solution<sup>6,7</sup> is associated with values of  $\chi_1 \sim -60^\circ, \chi_2 \sim +90^\circ$ . Corresponding values for methyl *N*-acetyl-L-tryptophanate crystallized from methanol<sup>8</sup> are  $\chi_1 \sim -65^\circ, \chi_2 \sim 88^\circ$ . This is also the predominant conformation of the side chain of L-tryptophan in proteins.<sup>2,15</sup>

(15) In ref 2b the rotamer of L-tryptophan designated as  $g^+$  corresponds to that designated as  $g^-$  according to: IUPAC-IUB Commission on Biochemical Nomenclature *Biochemistry* 1970, 9, 3471-3479.

**Table III.** Comparison of Dihedral Angles of ENDOR Compatible Conformations of the Tryptophan Side Chain of Methyl *N*-(2,2,5,5-Tetramethyl-1-oxypyrrolinyl-3-carbonyl)-L-tryptophanate and of the Reference Molecular Model

dihedral angles	ref molec model <sup>a</sup>	conformations found <sup>b</sup>			methyl L-alanate <sup>c</sup>
		"extended"		"closed"	
		A	B	C	
Without Hydrogen Atoms					
[C(4)-C(3)-C(6)-O(2)]	149	138 ± 2	138 ± 2	130 ± 5	146 ± 5
[C(4)-C(3)-C(6)-N]	-31	-42 ± 2	-42 ± 2	-50 ± 5	-35 ± 5
[C(3)-C(6)-N-C <sup>α</sup> ]	-177	-176 ± 2	-176 ± 2	-177 ± 3	-170 ± 4
[O(2)-C(6)-N-C <sup>α</sup> ]	4	4 ± 2	4 ± 2	3 ± 3	9 ± 4
[C(6)-N-C <sup>α</sup> -C]	-68	-66 ± 6	-66 ± 6	-87 ± 7	-93 ± 12
[C(6)-N-C <sup>α</sup> -C <sup>β</sup> ]	170	172 ± 6	172 ± 6	151 ± 7	144 ± 12
[N-C <sup>α</sup> -C <sup>β</sup> -C <sup>γ</sup> ]	-65	-63 ± 2	-63 ± 2	-95 ± 5	
[C-C <sup>α</sup> -C <sup>β</sup> -C <sup>γ</sup> ]	173	174 ± 2	174 ± 2	142 ± 5	
[C <sup>α</sup> -C <sup>β</sup> -C <sup>γ</sup> -C <sup>δ1</sup> ]	88	105 ± 5	-33 ± 5	-105 ± 8	
[C <sup>α</sup> -C <sup>β</sup> -C <sup>γ</sup> -C <sup>δ2</sup> ]	-90	-73 ± 5	150 ± 5	77 ± 8	
With Hydrogen Atoms					
[O(2)-C(6)-N-H <sup>N</sup> ]	-176	-176 ± 2	-176 ± 2	-177 ± 3	-171 ± 4
[C(3)-C(6)-N-H <sup>N</sup> ]	3	4 ± 2	4 ± 2	-16 ± 3	10 ± 4
[H <sup>N</sup> -N-C <sup>α</sup> -H <sup>α</sup> ]	-129	-127 ± 6	-127 ± 6	-148 ± 7	-154 ± 12
[H <sup>N</sup> -N-C <sup>α</sup> -C <sup>β</sup> ]	-10	-8 ± 6	-8 ± 6	-29 ± 7	-36 ± 12
[N-C <sup>α</sup> -C <sup>β</sup> -H <sup>β1</sup> ]	175	177 ± 2	177 ± 2	145 ± 5	172 ± 5
[C-C <sup>α</sup> -C <sup>β</sup> -H <sup>β1</sup> ]	52	54 ± 2	54 ± 2	23 ± 5	50 ± 5
[H <sup>α</sup> -C <sup>α</sup> -C <sup>β</sup> -H <sup>β1</sup> ]	-67	-66 ± 2	-66 ± 2	-97 ± 5	-70 ± 5
[H <sup>α</sup> -C <sup>α</sup> -C <sup>β</sup> -C <sup>γ</sup> ]	53	55 ± 2	55 ± 2	24 ± 5	
[H <sup>β1</sup> -C <sup>β</sup> -C <sup>γ</sup> -C <sup>δ1</sup> ]	-152	-135 ± 5	87 ± 5	15 ± 8	
[H <sup>β1</sup> -C <sup>β</sup> -C <sup>γ</sup> -C <sup>δ2</sup> ]	30	45 ± 5	-91 ± 5	-162 ± 8	

<sup>a</sup> Atomic coordinates of the reference molecular model were derived from X-ray-defined fragments,<sup>8,13</sup> as discussed in the text. Values of dihedral angles are given in degrees. <sup>b</sup> Three conformations were found for the tryptophan side chain, as illustrated in Figure 7. <sup>c</sup> Corresponding values of the spin-labeled methyl L-alanate analogue from ref 5.

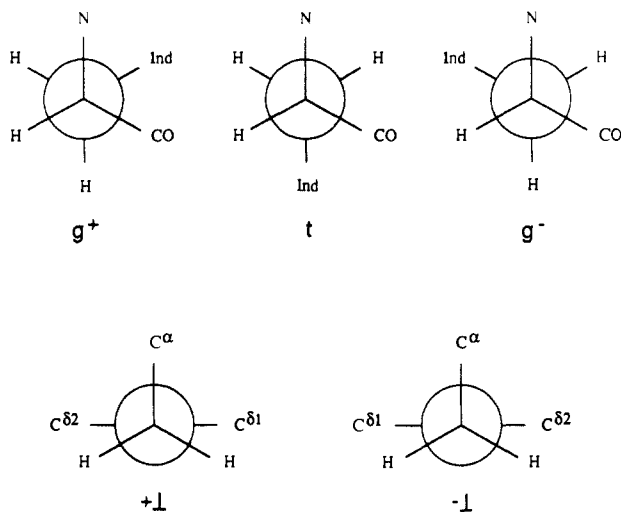


**Figure 8.** Newman diagrams of the gauche<sup>+</sup> (g<sup>+</sup>), trans (t), and gauche<sup>-</sup> (g<sup>-</sup>) conformations of L-tryptophan. The dihedral angle relationships for  $\chi_1$  are shown in the upper part while the relationships for  $\chi_2$  indicating perpendicular (+ $\perp$ ) and antiperpendicular (- $\perp$ ) conformations are shown in the lower part.

In Figure 9 we have illustrated angle maps of  $\chi_1$  and  $\chi_2$  calculated according to the ENDOR-determined distance constraints of the spin-labeled methyl L-tryptophanate molecule in "extended" and "closed" conformations. The electron-proton and electron-fluorine distances provide the effective spectroscopic probe of the angle  $\chi_1$  while the <sup>19</sup>F resonances primarily serve as the spectroscopic monitor of the angle  $\chi_2$ . As seen in Figure 9, we have calculated these maps separately for the  $\eta^2$ -fluoro- and the  $\zeta^3$ -fluorotryptophan analogues for which only one electron-fluorine distance constraint is applied together with corresponding distance constraints to H<sup>α</sup>, H<sup>β1</sup>, and H<sup>β2</sup>. In view of the identical electron-proton distance constraints for both types of fluorine-substituted derivatives, we have also compared these results in Figure 9 to the case in which both sets of electron-fluorine separations were applied together to a hypothetical  $\eta^2, \zeta^3$ -difluorotryptophan derivative. This calculation assigns the conformational space compatible with both fluorine-substituted derivatives simultane-

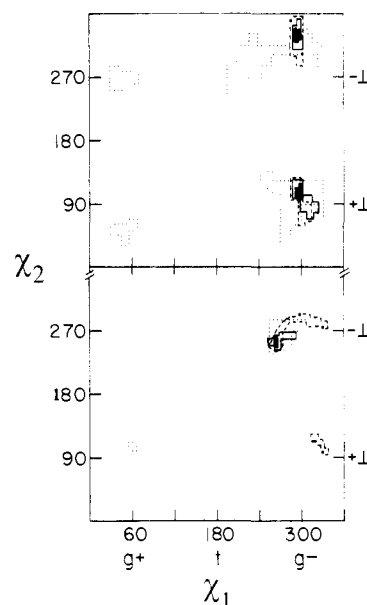


**Figure 9.** The angle maps of  $\chi_1$  and  $\chi_2$  for conformers A and B (upper panel) and for conformer C (lower panel) of spin-labeled methyl tryptophanate as a function of ENDOR-determined distance constraints. The axes representing values of  $\chi_1$  and  $\chi_2$  are indicated in degrees. The values of  $\chi_1$  and  $\chi_2$  are labeled on the axes of the classical rotamers illustrated in Figure 8. The conformational space is represented by solid lines for the F<sup>3</sup> isomer and by dashed lines for the F<sup>2</sup> isomer. The filled area represents the ENDOR compatible space obtained by simultaneous application of the distance constraints to F<sup>3</sup> and F<sup>2</sup>. We have also illustrated with dotted lines the conformational space calculated with an uncertainty in the electron-nucleus distances of 10% of the measured values of  $r$ . For this calculation distance constraints to F<sup>3</sup>, F<sup>2</sup>, and all protons were simultaneously applied.

ously and reduces the conformational space that arises as ENDOR compatible because of line width based uncertainties. The results in Figure 9 show that the ENDOR compatible conformations are clustered around values of  $\chi_1 \sim -60^\circ$  for conformers A and B and around  $\chi_1 \sim -95^\circ$  for conformer C. These values of  $\chi_1$  belong to the g<sup>-</sup> rotamer classification. The distance constraints rule out

entirely occurrence of the  $g^+$  ( $\chi_1 \sim +60^\circ$ ) and the  $t$  ( $\chi_1 \sim 180^\circ$ ) rotamers under the solvent and temperature conditions employed for preparation of samples in these studies.

The conformational analysis of tryptophan derivatives in solution has been largely carried out on the basis of NMR methods through measurements of vicinal coupling constants<sup>7</sup> and of internucleus distances by nuclear Overhauser effects or perturbation of nuclear spin-lattice relaxation rates by paramagnetic ions.<sup>6</sup> The NMR data are analyzed in terms of all six conformers of the side chain and frequently do not permit easily assignment of the conformer of greatest population. In NMR studies the uncertainties associated with estimates of internucleus separations are much greater than those obtained in this study by ENDOR. To illustrate the importance of the relative magnitude of the uncertainties associated with estimates of electron-nucleus separations to assign conformation, we have also compared in Figure 9 the ENDOR compatible conformational space with that obtained by increasing the error to a hypothetical value of  $\sim 10\%$  of the measured value of  $r$ . With the application of these larger distance uncertainties, as would be obtained, for instance, in nuclear Overhauser experiments,<sup>4,6,16</sup> the  $t$  rotamer ( $\chi_1 \sim 180^\circ$ ) would be compatible with the ENDOR data for conformers A and B while the  $g^+$  rotamer ( $\chi_1 = +60^\circ$ ) would be compatible for all three conformers A, B, and C. However, these regions of conformational space near  $\chi_1 = +60$  and  $180$  occur only for values of ( $r \pm \Delta r$ ) with large uncertainties. These regions do not apply to the more precise ENDOR results provided in Tables I and II.

Since the  $g^+$  and  $t$  rotamers are excluded by the precision of the ENDOR-determined values of electron-nucleus separations and since the proton ENDOR spectra indicated precisely identical ENDOR splittings for each class of protons in esters of L-tryptophan,  $\eta$ 2-fluorotryptophan, and  $\zeta$ 3-fluorotryptophan, our further conformational analysis is based on simultaneous application of the electron-fluorine separations for the  $\eta$ 2-fluoro- and the  $\zeta$ 3-fluoro-substituted analogues. These constraints on the torsion angle search calculations, thus, limit the possible conformations of the "extended" form to values of  $\chi_1 \sim -63^\circ$ , belonging to the  $g^-$  rotamer. The value of  $\chi_2$  compatible with the ENDOR distance constraints for conformer A is  $\sim +105^\circ$ , close to that of  $+90^\circ$  characteristic of the classical perpendicular conformation. For conformer B,  $\chi_2 \sim -33^\circ$ . This latter rotamer results in a nearly eclipsed configuration about the  $C^\beta-C^\gamma$  bond. We believe that this conformation would be of sufficiently higher potential energy to render conformer B of low population.<sup>17</sup> We, therefore, conclude that the only "extended" conformer that exists under the conditions of our ENDOR studies is conformer A with dihedral angles as summarized in Table III and illustrated in Figure 7. On the other hand, the ENDOR data for conformer C of spin-labeled methyl tryptophanate in chloroform/toluene, as seen in Figure 9, restrict the value of  $\chi_1$  to  $\sim -95^\circ$ , near that of the classical  $g^-$  ( $\chi_1 \sim -60^\circ$ ) rotamer. Correspondingly, for this conformer, the value of  $\chi_2 \sim -105^\circ$  is close to that of the classical antiperpendicular rotamer ( $\chi_2 \sim -90^\circ$ ).

For conformer A with  $\chi_1 \sim -63^\circ$ ,  $\chi_2 \sim +105^\circ$ , as summarized in Table III, the proton ENDOR data show that the dihedral angles involving hydrogens, particularly  $[N-C^\alpha-C^\beta-H^{\beta 1}]$ ,  $[C-C^\alpha-C^\beta-H^{\beta 1}]$  and  $[H^\alpha-C^\alpha-C^\beta-C^{\beta 1}]$  are close to the classical values of  $180$ ,  $60$ , and  $-60^\circ$ . On the other hand, conformer C is achieved both by a rotation around the  $C^\alpha-C^\beta$  bond to  $\chi_1 \sim -95^\circ$  and by a rotation around the  $C^\beta-C^\gamma$  bond to produce a near antiperpendicular orientation ( $\chi_2 \sim -105^\circ$ ) of the indole ring. This is also confirmed by the dihedral angle values in Table III in which the  $[N-C^\alpha-C^\beta-H^{\beta 1}]$ , ...,  $[C-C^\alpha-C^\beta-H^{\beta 1}]$  dihedral angles differ

by  $\sim -30^\circ$  from their conformer A counterparts. Conformer C described here on the basis of ENDOR data, thus, differs distinctly from all classical rotamers previously considered for tryptophan derivatives. Although this conformation has not been previously identified in other spectroscopic studies, the ENDOR data demonstrate that under certain solvent conditions, i.e., chloroform/toluene, this is the predominant conformation of spin-labeled methyl *N*-tryptophanate.

The existence of multiple conformers of tryptophan derivatives has been confirmed by a variety of physical methods, including NMR,<sup>6,7</sup> fluorescence decay,<sup>19</sup> and supersonic jets.<sup>20</sup> In NMR studies of tryptophan and of mono- and ditryptophanyl derivatives in alkaline methanol, it has been shown that the fraction of the  $g^-$  rotamer for Gly-Trp and Gly-Trp-Gly increases with decreasing temperature, and at  $-64^\circ\text{C}$ , for instance, 80% of the tripeptide Gly-Trp-Gly is found as the  $g^-$  rotamer.<sup>7b,c</sup> This is in agreement with our determination of the population of I as belonging to  $g^-$  at  $-100^\circ\text{C}$ , the freezing point of methanol. Although tryptophan, Trp-Gly, and ditryptophanyl derivatives show by NMR other types of temperature-dependent rotamer distributions, the Gly-Trp and Gly-Trp-Gly species probably model more accurately the behavior of spin-labeled methyl L-tryptophanate because of the peptide bond at the amino terminal side of the side chain.

The fluorescence emission of the indole ring in tryptophan exhibits two decay processes that are kinetically distinct on the picosecond time scale.<sup>19</sup> For these experiments, carried out at ambient room temperature, it has been suggested that the molecules are equilibrated with respect to  $\chi_1$ , and that the two decay processes are due separately to the perpendicular ( $\chi_2 = +90^\circ$ ) and antiperpendicular ( $\chi_2 = -90^\circ$ ) rotamers around the  $C^\beta-C^\gamma$  bond. This rotameric change results in different environments of the indole ring with respect to the amine and carboxylate groups that could influence the electronic properties of the indole ring through electrostatic effects.<sup>19b,c</sup> Our results support this hypothesis, showing that conformers A and C of spin-labeled methyl L-tryptophanate are characterized by  $\chi_1$  values near that of the  $g^-$  rotamer but by values of  $\chi_2$  corresponding closely to classical perpendicular and antiperpendicular rotamers. This difference in orientation of the indole ring is, thus, consistent with the postulated effect to result in two different fluorescence decay processes. Since the relative populations of conformers A and C depend on solvent polarity, as shown in our studies, a solvent-dependence study of the fluorescence decay properties of tryptophan derivatives may be able to identify which of these two structural conformers is responsible for the slow and which is responsible for the fast decay process observed on the picosecond time scale.

The predominant conformation of the side chain of I in a nonpolar solvent is essentially that of the  $g^-$  conformer with  $\chi_1 \sim -95^\circ$  but with an antiperpendicular orientation of the indole ring ( $\chi_2 = -105^\circ$ ). By changing the solvent to methanol, the population of this conformer is greatly reduced, with appearance of a new conformer that differs primarily according to the  $\chi_2$  dihedral angle to yield a perpendicular orientation of the side chain. Thus, an interesting observation from these ENDOR studies is the change in relative population of conformers with change in solvent. Since the freezing temperatures of the two solvent systems employed in this investigation are approximately both  $-100^\circ\text{C}$ ,<sup>21</sup> the difference in conformer population cannot be ascribed to a temperature-dependent equilibrium between conformers A and C. Therefore, we believe that the interactions between the solvent

(16) (a) Havel, T. F.; Wüthrich, K. *J. Mol. Biol.* **1985**, *182*, 281-294. (b) Williamson, M. P.; Havel, T. F.; Wüthrich, K. *J. Mol. Biol.* **1985**, *182*, 295-315. (c) Wüthrich, K.; Billeter, M.; Braun, W. *J. Mol. Biol.* **1984**, *180*, 715-740. (d) Wüthrich, K.; Billeter, M.; Braun, W. *J. Mol. Biol.* **1983**, *169*, 949-961.

(17) Estimates of the barrier to rotation in tyrosine and phenylalanine show that a conformer with  $\chi_2 \sim \pm 30^\circ$  is 4-5 kcal/mol above that with  $\chi_2 \sim \pm 90^\circ$ .<sup>18</sup>

(18) Umeyama, H.; Nakagawa, S. *Chem. Pharm. Bull.* **1979**, *27*, 2227-2228.

(19) (a) Robbins, R. J.; Fleming, G. R.; Beddard, G. S.; Robinson, G. W.; Thistlethwaite, P. J.; Woolfe, G. J. *J. Am. Chem. Soc.* **1980**, *102*, 6271-6279. (b) Engh, R. A.; Chen, L. X. Q.; Fleming, G. R. *Chem. Phys. Lett.* **1986**, *126*, 365-372. (c) Chen, L. X. Q.; Engh, R. A.; Fleming, G. R. *J. Phys. Chem.* **1988**, *92*, 4811-4816.

(20) (a) Rizzo, T. R.; Park, Y. D.; Levy, D. H. *J. Am. Chem. Soc.* **1985**, *107*, 277-278. (b) Rizzo, T. R.; Park, Y. D.; Peteanu, L. A.; Levy, D. H. *J. Chem. Phys.* **1986**, *84*, 2534-2541. (c) Park, Y. D.; Rizzo, T. R.; Peteanu, L. A.; Levy, D. H. *J. Chem. Phys.* **1986**, *84*, 6539-6549.

(21) Timmermans, J. *The Physico-chemical Constants of Binary Systems in Concentrated Solutions*; Interscience Publishers Inc.: New York, 1959; Vol. 1, p 273.



**Table IV.** Geometric Relationships and Estimated Interaction Energies of the Dipoles of the Peptide Bond and the Indole Ring in Spin-Labeled Methyl L-Tryptophanate<sup>a</sup>

conformer	angle, deg	dipole-dipole sepn, Å	dipolar energy, <sup>b</sup> kcal/mol	fraction <sup>c</sup>
A	35	4.83	+0.73	0.02
B	120	5.10	-0.34	
C	121	4.93	-0.56	0.98

<sup>a</sup> Calculated for point dipoles, as described in 3-methylindole<sup>24</sup> and for the peptide bond.<sup>22,23</sup> <sup>b</sup> Calculated for the molecule in vacuo. <sup>c</sup> Calculated at -100 °C to approximate the freezing temperatures<sup>21</sup> of the solvents employed; conformer B is not included in the estimation of relative conformer populations because no spectroscopic evidence was observed for its existence in chloroform/toluene, as discussed in the text.

and the spin-labeled tryptophanate molecule must be of importance in conformer stabilization.

We suggest that the solvent dependence of the relative populations of the two conformers can be explained in terms of the interactions of the dipole moment of the peptide bond with that of the indole ring. It is well-known that the peptide bond is associated with a strong electric dipole moment of approximately 3.7 D.<sup>22,23</sup> Experimental and theoretical determinations of the value and direction in the dipole moments of indole and of its derivatives<sup>24-26</sup> have shown that the net dipole moment of the indole

ring of 2.13 D is directed from the center of the C<sup>2</sup>-C<sup>62</sup> bond toward N<sup>1</sup> (see Figure 1 for atom labeling), with the nitrogen associated with the positive end of the dipole. Applying the dipoles as described for 3-methylindole<sup>24</sup> and the peptide bond,<sup>22</sup> we have estimated their interaction energies for the conformers illustrated in Figure 7. The results are summarized in Table IV. For conformer C the two dipoles are oriented approximately anti-parallel, while in conformer A the dipoles are more nearly parallel. Based on the calculated dipolar interaction energy alone, conformer C is, thus, expected to be of greater population. On the other hand, the unfavorable dipolar interaction energy calculated for conformer A will be effectively reduced through hydrogen-bonding interactions of the indole ring and peptide group with methanol or through the higher dielectric screening effect of methanol over that of chloroform/toluene. On this basis, both conformers A and C may be expected to be present in methanol, as is, indeed, observed. It is of interest also to note that by calculation conformer B would be favored by the indole-peptide dipolar interaction in a solvent of low dielectric constant. The absence of a detectable fraction of this conformer in chloroform/toluene that would be characterized by an approximate 10-Å electron-fluorine separation (cf., Table II) supports our conclusion made earlier that conformer B is energetically unfavorable relative to conformers A and C.

**Registry No.** I, 125250-24-0; unlabeled I, 106367-36-6; II, 125250-25-1; III, 125250-26-2; IV, 125250-27-3; V, 125250-28-4; VI, 125250-29-5; VII, 125250-30-8; VIII, 125250-31-9; H-D-Trp-OH, 153-94-6; Ac-DL-( $\alpha$ -<sup>2</sup>H)Trp-OH, 80525-43-5; H-( $\alpha$ -<sup>2</sup>H)Trp-OH, 81279-11-0; H-Trp-OMe-HCl, 7524-52-9; 2,2,5,5-tetramethyl-1-oxypyrroline-3-carboxylic acid, 2154-67-8.

(22) Hol, W. G. J.; van Duijnen, P. T.; Berendsen, H. J. C. *Nature* **1978**, *273*, 443-446.

(23) Wada, A. *Adv. Biophys.* **1976**, *9*, 1-63.

(24) Párkányi, C.; Oruganti, S. R.; Abdelhamid, A. O.; von Szentpály, L.; Ngom, B.; Aaron, J.-J. *J. Mol. Struct.* **1986**, *135*, 105-116.

(25) Weiler-Feilchenfeld, H.; Pullman, A.; Berthod, H.; Giessner-Prettre, C. *J. Mol. Struct.* **1970**, *6*, 297-304.

(26) Sun, M.; Song, P. S. *Photochem. Photobiol.* **1977**, *25*, 3-9.

## Elimination of Cross-Relaxation Effects from Two-Dimensional Chemical-Exchange Spectra of Macromolecules

Jasna Fejzo,<sup>†,‡</sup> William M. Westler,<sup>‡</sup> Slobodan Macura,<sup>†</sup> and John L. Markley<sup>\*,‡</sup>

Contribution from the Institute of Physical Chemistry, University of Belgrade, 11000 Beograd, P.O. Box 550, Yugoslavia, and Department of Biochemistry, College of Agricultural and Life Sciences, University of Wisconsin—Madison, 420 Henry Mall, Madison, Wisconsin 53706. Received June 12, 1989

**Abstract:** We demonstrate here a method for eliminating cross-relaxation effects from exchange spectra of macromolecules that permits a more rigorous study of chemical-exchange processes. In the spin diffusion limit, the laboratory-frame cross-relaxation rate is negative and equal to half the rotating-frame cross-relaxation rate, which is positive. If, during the mixing time, the magnetization is flipped rapidly between the two frames such that the average residence time in the NOESY:ROESY frames is 2:1, then the magnetization exchange due to cross-relaxation will cancel out and be removed. Since chemical exchange takes place steadily, irrespective of the frame of reference, it will contribute to cross-peak volumes in the usual manner. This approach has been applied to the elimination of cross-relaxation effects from the 2D exchange spectrum of a small globular protein, turkey ovomucoid third domain (6062 Da). The results demonstrate that tyrosine-31 executes ring flips on the millisecond time scale.

Two-dimensional (2D) exchange spectroscopy<sup>1,2</sup> has become a popular method for investigating molecular structure and dynamics. The method provides information on incoherent magnetization transfer among spins due to chemical exchange and cross-relaxation. These two processes are independent and can occur simultaneously. In order to analyze 2D exchange spectra,

one needs to distinguish and evaluate the magnetization transfer that occurs by these two different mechanisms. In NOESY spectra of macromolecules, cross-relaxation and chemical exchange are indistinguishable because they both give rise to positive cross-peaks.<sup>3</sup> In ROESY spectra of macromolecules direct

\* To whom correspondence should be addressed.

<sup>†</sup> University of Belgrade.

<sup>‡</sup> University of Wisconsin—Madison.

(1) Jeener, J.; Meier, B. H.; Bachman, P.; Ernst, R. R. *J. Chem. Phys.* **1979**, *71*, 4546-4553.

(2) Ernst, R. R.; Bodenhausen, G.; Wokaun, A. *Principles of NMR in One and Two Dimensions*; Clarendon Press: Oxford, 1987.